Mol Divers (2017) 21:967–983
DOI 10.1007/s11030-017-9776-1

ORIGINAL ARTICLE

Synthesis, characterization and molecular docking studies of thiouracil derivatives as potent thymidylate synthase inhibitors and potential anticancer agents

Abeer M. El-Naggar[1] · Mohsen M. Abou-El-Regal[1] · Souad A. El-Metwally[2] · Farag F. Sherbiny[3,4] · Ibrahim H. Eissa[5]

Received: 27 March 2017 / Accepted: 2 August 2017 / Published online: 16 August 2017

Abstract Thymidylate synthase (TS), one of folate-dependent enzymes, is a key and well-recognized target for anticancer agents. In this study, a series of 6-aryl-5-cyano thiouracil derivatives were designed and synthesized in accordance with essential pharmacophoric features of known TS inhibitors. Nineteen compounds were screened in vitro for their anti-proliferative activities toward HePG-2, MCF-7, HCT-116, and PC-3 cell lines. Compounds **21$_c$**, **21$_d$**, and **24** exhibited high anti-proliferative activity, comparable to that of 5-fluorouracil. Additionally, ten compounds with potent anti-proliferative activities were further evaluated for their ability to inhibit TS enzyme. Six compounds (**21$_b$**, **21$_c$**, **21$_d$**, **22**, **23** and **24**) demonstrated potent dose-related TS inhibition with IC_{50} values ranging from 1.57 to 3.89 μM. The in vitro TS activity results were consistent with those of the cytotoxicity assay where the most potent anti-proliferative compounds of the series showed good TS inhibitory activity comparable to that of 5-fluorouracil. Furthermore, molecular docking studies were carried out to investigate the binding pattern of the designed compounds with the prospective target, TS (PDB-code: 1JU6).

Keywords Anticancer · Thymidylate synthase · 6-Aryl-5-cyano thiouracil · Docking

Electronic supplementary material The online version of this article (doi:10.1007/s11030-017-9776-1) contains supplementary material, which is available to authorized users.

✉ Abeer M. El-Naggar
elsayedam@sci.asu.edu.eg

✉ Ibrahim H. Eissa
Ibrahimeissa@azhar.edu.eg

1 Chemistry Department, Faculty of Science, Ain Shams University, Abbassia, Cairo 11566, Egypt

2 Higher Technology Institute, 10th of Ramadan City, Egypt

3 Organic Chemistry Department, Faculty of Pharmacy (Boys), Al-Azhar University, Cairo 11884, Egypt

4 Organic Chemistry Department, Faculty of Pharmacy, October University for Modern Science and Arts (MSA), 11787 6th October City, Egypt

5 Pharmaceutical Chemistry Department, Faculty of Pharmacy (Boys), Al-Azhar University, Cairo 11884, Egypt

Introduction

Cancer is a prime public health problem all over the world [1]. It initiates when cells in a part of the body start to grow without control [2]. Cancer is the second main cause of death in the USA [3]. Today, millions of people are living with cancer [3]. Approximately 13% of all deaths worldwide, numbering 8.2 million people annually, are due to cancer. Currently, more than 100 cancer types exist and each needs unique diagnosis and treatment [4,5].

Thymidylate synthase (TS), a folate-dependent enzyme, is a key well-recognized target for anticancer agents. Due to its crucial role in DNA synthesis, it is an important enzyme in all body functions [6]. The main role of TS lies in its dual function; it acts as a catalytic enzyme and as an effective regulator of its own expression by binding and inactivating its own RNA. With regard to its catalytic function, it catalyzes the reductive methylation of 2′-deoxyuridine-5′-monophosphate (dUMP) to 2′-deoxythymidine-5′-monophosphate (dTMP) [7]. The regulatory role of TS may be implicated in the synthesis of key proteins that regulate the apoptotic process [8].

TS inhibitors bind to TS through two main essential moieties: pyrimidine and glutamate. The pyrimidine moiety binds to a pyrimidine-binding site, while the glutamate moiety binds to a folate-binding site [9,10].

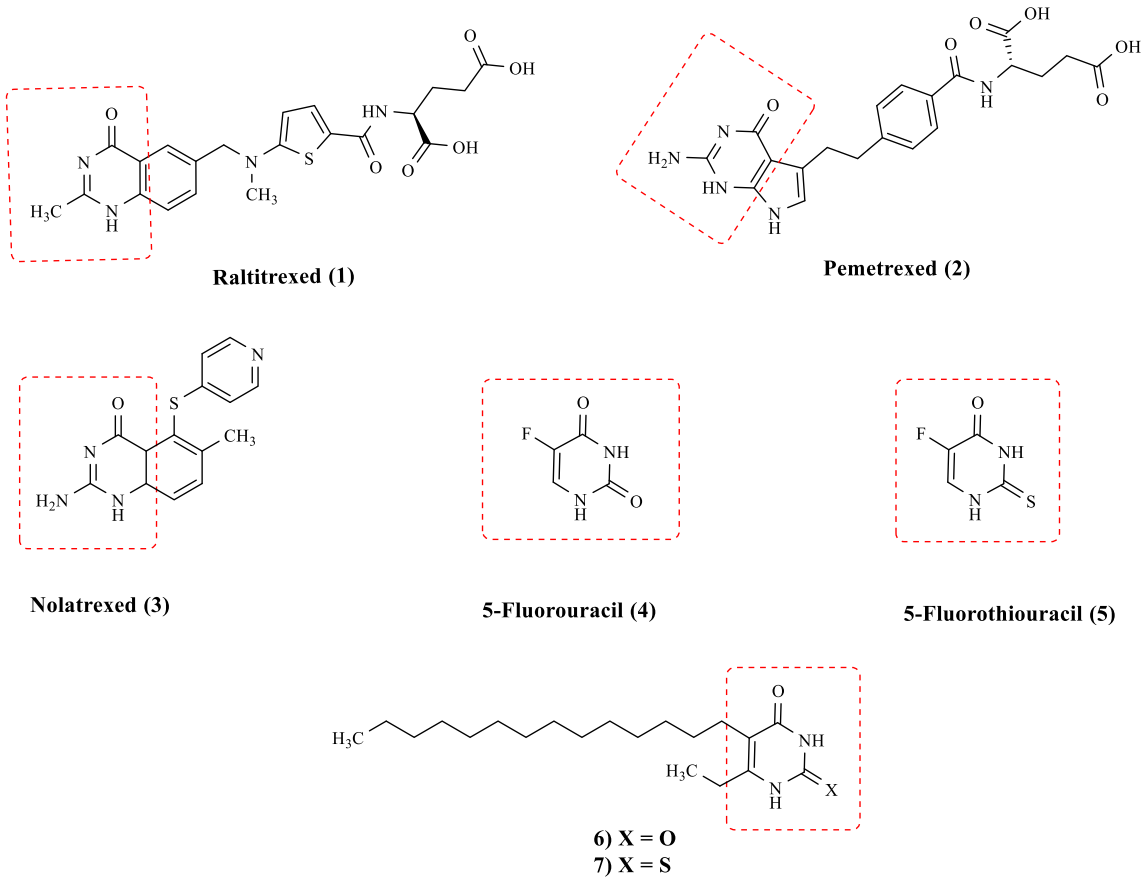

Fig. 1 Structures and basic pharmacophoric features of some reported TS inhibitors

5-Fluorouracil (5-FU) **4** and its modified analogue, 5-fluorothiouracil **5**, are widely used anticancer agents [11–13]. These drugs can be inserted into RNA and/or DNA resulting in interference with the maturation of nuclear RNA and/or DNA. However, the main mechanism of action of fluorouracil is its conversion into 5-fluoro-2′-deoxy-5′-monophosphate (FdUMP) resulting in inhibition of TS and DNA synthesis [10]. 5-FU treatment has various adverse effects, including (i) toxic side effects due to its misincorporation into RNA, (ii) resistance often developed due to a decrease in kinases cellular levels required for metabolic activation, and (iii) as a single antineoplastic agent, it has a narrow range of activity [9]. Macchia et al. [14] designed and synthesized compounds **6** and **7**, modified analogues of 5-fluorouracil and 5-fluorothiouracil, respectively. These compounds were screened for anti-proliferating in vitro and in vivo anti-tumor activity. These compounds showed promising anticancer activity with IC_{50} values of 7.9 and 1.7 μM, respectively.

The crystal structures of TS from mammalian and bacterial sources provided key information [15] to design and synthesize new TS inhibitors, e.g., raltitrexed **1** [16], pemetrexed **2** [17] and nolatrexed **3** [18]. Raltitrexed **1** and pemetrexed **2** contain glutamate moieties that can bind to the enzyme at both folate- and pyrimidine-binding sites. The new non-classical generation of TS-directed inhibitors such as nolatrexed **3** is lacking a negatively charged glutamate side chain. The design of this TS inhibitor is based on computer-assisted design using high-resolution X-ray crystallography [19–22].

Based on the previously mentioned findings, we decided to design and synthesize a novel series of thiouracils incorporating a nitrile group instead of the fluoro group. The synthesized compounds were designed to contain a pyrimidine moiety, the main and essential pharmacophoric feature of TS inhibitors, with the major target of developing agents with potential anticancer activity that could be more effective than 5-fluorouracil.

Rationale of molecular design

Many reported facts were clarified before the chemical synthesis of our target compounds. The first fact was the presence of a pyrimidine nucleus is essential as a basic pharmacophoric feature for TS inhibition [23]. The second fact was modifications at the fifth and sixth positions of 5-fluorouracil and 5-fluorothiouracil led to the generation of many TS inhibitors such as compounds **6** and **7** with potent anticancer activities [14] (Fig. 1). The third fact was the existence

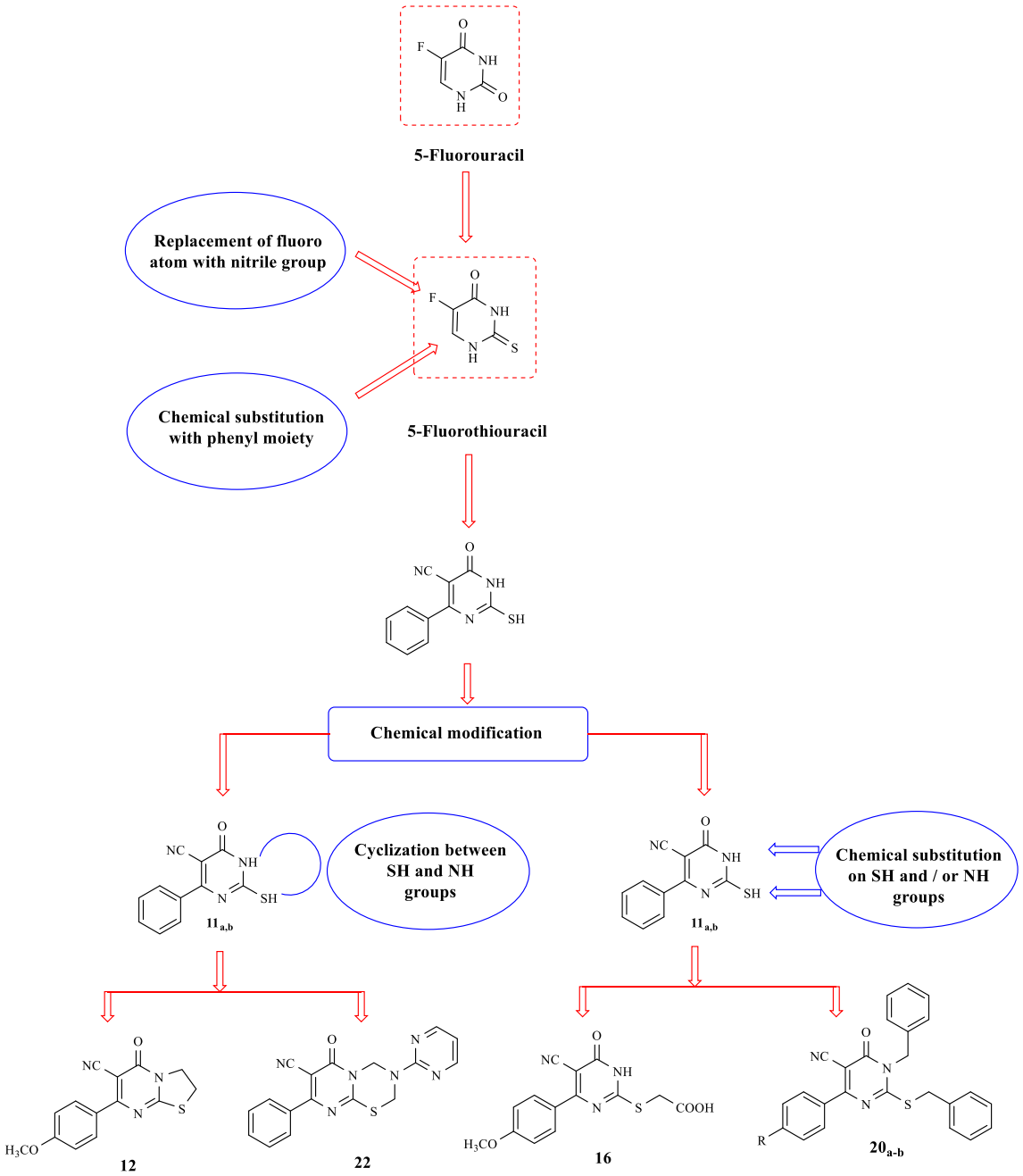

Fig. 2 Rationale of molecular design of new anticancer agents

of new non-classical generation of TS inhibitors without a negatively charged glutamate side chain [24]. Based on all this information, ligand-based drug design approach was achieved to improve chemotherapeutic activity of these inhibitors.

The main core of our molecular design rationale comprises chemical modifications on 5-fluorothiouracil at four different positions (Fig. 2). The first position is C5, with the replacement of a fluoro group with isosteric nitrile group. This modification was based on several bioisosteric considerations: (i) The nitrile group has a crucial role as hydrogen bond acceptor [25,26]. Many publications reported that nitrile protrudes into strict active sites to form an important polar hydrogen bonding interaction [27]; (ii) the nitrile may increase the polar character of the aromatic π-system [28]; (iii) moreover, the nitrile group may not engage in specific interactions, but may enhance pharmacokinetic properties. Solubility studies of farnesyltransferase inhibitors revealed that nitrile-containing members were nearly tenfold more soluble than the corresponding bromo analogues [29].

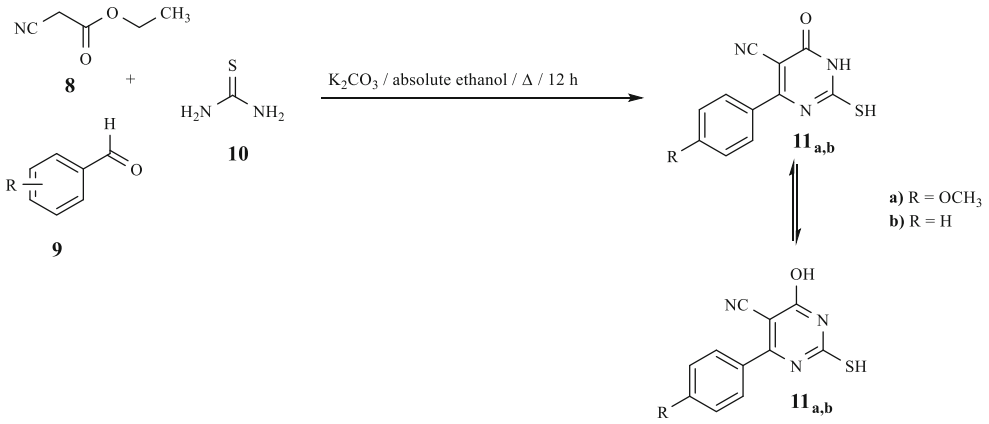

Scheme 1 General procedure for synthesis of target compounds $\mathbf{11_{a,b}}$

The second position is C6 through phenyl substitution. The insertion of a phenyl group may increase binding affinity since the synthase enzyme is very large and contains a deep pocket for the binding of both substrate and cofactor [30]. The third and fourth positions are N-3 heteroatom and the SH group with three pathways of modifications: (i) chemical substitutions on the SH moiety with different alkyl and aralkyl moieties, (ii) chemical substitutions on both N-3 atom and SH group with different alkyl and aralkyl moieties, and (iii) using N-3 and SH groups to form five- or six-membered rings.

This rationale of molecular design allowed the generation of new hybrid structures with different biological isosteres. The wide variety of chemical modifications may help us to study the SAR of these novel compounds as anticancer agents. The binding mode of 5-fluorouracil with the active site of TS has been unequivocally elucidated [31,32]. Based on this information, we carried out molecular docking studies to confirm the binding manner as well as the inhibitory activity of the synthesized compounds toward TS.

Results and discussion

Chemistry

The sequence of reactions used in the synthesis of the title compounds is shown in Schemes 1–4. The starting key compounds $\mathbf{11_{a,b}}$ were synthesized via a one-pot cyclocondensation reaction where equivalent molar quantities of aromatic aldehydes, ethyl cyanoacetate and thiourea reacted in absolute ethanol in the presence of anhydrous K_2CO_3 followed by neutralization with acetic acid [33] (Scheme 1).

Compound $\mathbf{11_a}$ reacted with commercially available 1,2-dibromoethane in the presence of anhydrous K_2CO_3 and tetrabutylammonium bromide (TBAB) in dry THF to afford cyclo-substitution product **12**. Compound $\mathbf{11_b}$ underwent a nucleophilic displacement reaction with acetyl chloride to give compound **13**. Furthermore, reaction of $\mathbf{11_a}$ with methylene chloride produced 2,2′-[methylenebis(sulfanediyl)]bis [4-(4-methoxyphenyl)-6-oxo-1,6-dihydropyrimidine-5-carbonitrile] **14** (Scheme 2).

S-Alkylation reactions were carried out between equimolar amounts of key compounds $\mathbf{11_{a,b}}$ and appropriate commercially available halo derivatives, namely allyl bromide, chloroacetic acid, ethyl chloroacetate, diethyl bromomalonate and ethyl chloroformate in the presence of anhydrous K_2CO_3 and tetrabutylammonium bromide in dry THF to give the corresponding thiouracil derivatives **15–19**, respectively. While the reaction of $\mathbf{11_{a,b}}$ with two molar equivalent of benzyl chloride gave di-benzylated carbonitriles $\mathbf{20_{a,b}}$ (Scheme 3).

Since Mannich reaction is a convenient method for the introduction of an amino methylene fragment in compounds bearing an acidic proton, we found compounds $\mathbf{11_{a,b}}$ are suitable substrates for such amino methylation process. Reaction of compounds $\mathbf{11_{a,b}}$ with one equivalent of an appropriate primary amine, namely 4-methoxyaniline, p-toluidine, 2-amino-pyrimidine, iso-butylamine and 2-naphthylamine, with excess of formaldehyde (37%) in dioxane produced the corresponding target compounds **21–24**, respectively (Scheme 4). The structures of all newly synthesized novel compounds were confirmed by spectral and elemental analyses.

Biological evaluation

In vitro anti-proliferative activity

In vitro evaluation of the newly synthesized compounds for their anti-proliferative activities was carried out against four human cancer cell lines, namely hepatocellular carcinoma (HePG-2), breast carcinoma (MCF-7), colorectal carcinoma (HCT-116) and prostate cancer (PC-3). The biological eval-

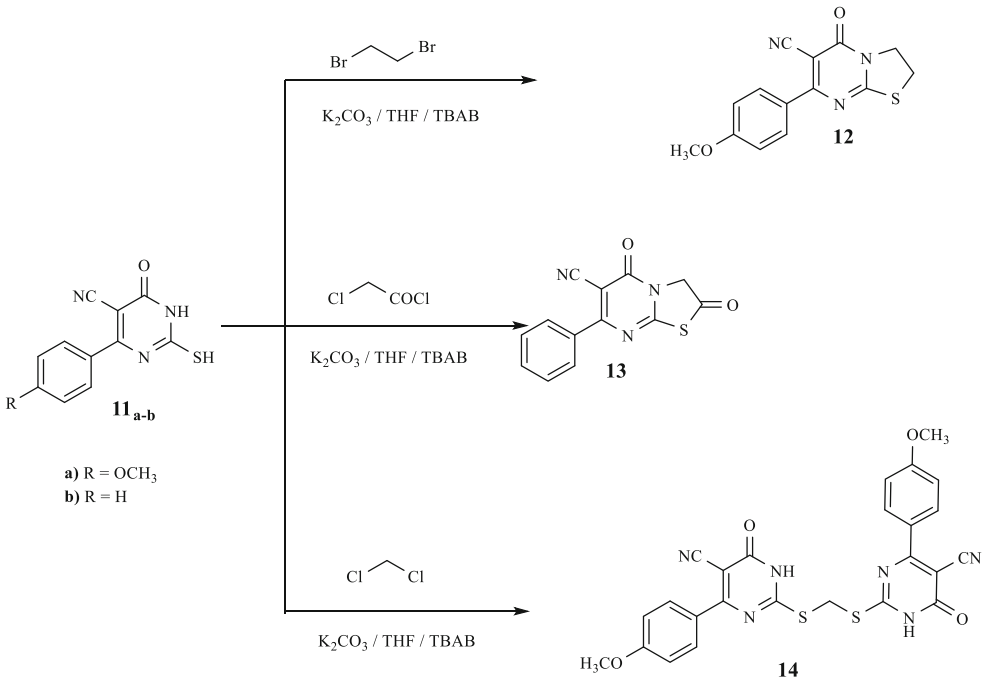

Scheme 2 General procedure for synthesis of target compounds **12–14**

uation was performed using a sulforhodamine B (SRB) colorimetric assay as described by Skehan et al. [34]. The cytotoxicity results were expressed as median inhibitory concentration (IC_{50}) values for the synthesized compounds using drug 5-fluorouracil as reference (Table 1).

The screened compounds showed different levels of cytotoxicity ranging from excellent, to moderate, to weak activities against the above 4 cell lines. In general, the best performers are compounds $\mathbf{21_c}$, $\mathbf{21_d}$ and **24**, of which compound **24** was the most potent one being 1.33, 1.28, 1.17, and 1.98 times more active than 5-fluorouracil against HePG-2 ($IC_{50} = 6.4 \pm 0.14\,\mu M$), MCF-7 ($IC_{50} = 5.9 \pm 0.11\,\mu M$), HCT-116 ($IC_{50} = 7.9 \pm 0.14\,\mu M$) and PC-3 ($IC_{50} = 5.2 \pm 0.09\,\mu M$), respectively.

Compounds **13**, $\mathbf{17_a}$, $\mathbf{17_b}$, $\mathbf{21_a}$, $\mathbf{21_b}$, **22** and **23** were found to possess moderate anti-proliferative activities with IC_{50} values ranging from 8.7 to 28.7 μM. The rest of the compounds were weaker inhibitors.

In vitro assay of thymidylate synthase (TS) activity

Compounds exhibiting anti-proliferative activities (**13**, $\mathbf{17_a}$, $\mathbf{17_b}$, $\mathbf{21_a}$, $\mathbf{21_b}$, $\mathbf{21_c}$, $\mathbf{21_d}$, **22**, **23** and **24**) were further evaluated to determine their inhibitory activities against thymidylate synthase (TS). The kinase activity of TS was measured spectrophotometrically according to reported procedure described by Wahba and Friedkin [35]. 5-Fluorouracil was used as a positive control in this assay. The results were reported as enzymatic inhibition percentage (%) and a 50% inhibition concentration values (IC_{50}) calculated from the concentration–inhibition response curve and are summarized in Table 1 and Fig. 3.

The tested compounds exhibited good to moderate inhibitory activity with IC_{50} values ranging from 1.57 to 14.04 μM, which were consistent with that of their in vitro cytotoxicity activities. 5-Fluorouracil as a reference compound showed 73.40% TS inhibition. Some of the test compounds exhibited higher activities than the reference standard (5-fluorouracil). Compounds $\mathbf{21_d}$ and **23** demonstrated potent inhibition, more than 80% for the TS activity with IC_{50} values of 1.57 ± 0.08 and $2.5 \pm 0.65\,\mu M$, respectively. In addition, significant inhibition above 70% was exhibited by several investigated compounds, namely $\mathbf{17_b}$, $\mathbf{21_b}$, **22** and **24**, with IC_{50} values of 5.13 ± 0.11, 3.66 ± 0.44, 3.51 ± 0.24 and $3.89 \pm 0.42\,\mu M$, respectively.

Molecular docking

In our work, docking of the synthesized compounds and reference ligands, 5-FU and LYA (co-crystallized ligand) with the TS crystal structure (ID: 1JU6), was carried to predict the binding mode, affinity and preferred orientation of each docking pose. The results of docking study are reported as TS binding free energy (ΔG) (Table 2).

The key binding site of TS has been reported [31,36] and involves amino acid residues of Phe225, Leu221 and Ile108. As reported, 5-FU was found to interact with two important

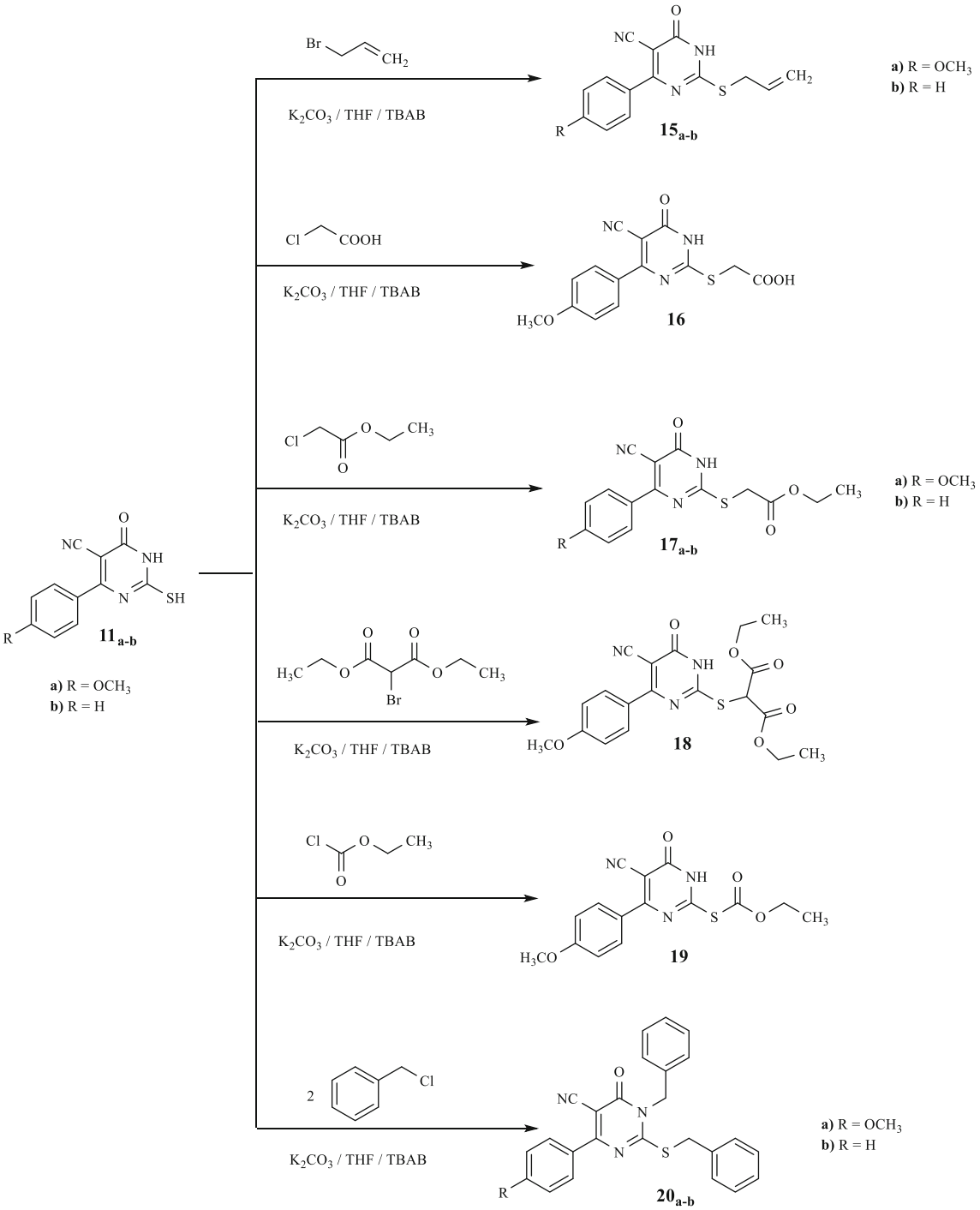

Scheme 3 General procedure for synthesis of target compounds $\mathbf{15_{a,b}}-\mathbf{20_{a,b}}$

amino acid residues of the active site (Leu221 and Phe225) [31].

The proposed binding mode of 5-FU showed an affinity value of −60.20 kcal/mol (RMSD = 1.20). The NH group at the 3-position was involved in a hydrogen bonding interaction with the carbonyl backbone of Ser216, the C=O group at the 2-position formed a hydrogen bond with side chain of Ser216, and the C=O group at the 4-position was involved in a hydrogen bonding interaction with Asn226. The aromatic moiety was involved in aromatic stacking interactions with Phe225 and Leu221 (Fig. 4).

The proposed binding mode of the re-docked co-crystallized ligand (LYA) showed affinity value of −90.32 kcal/mol. The side chain NH_2 group in position two was

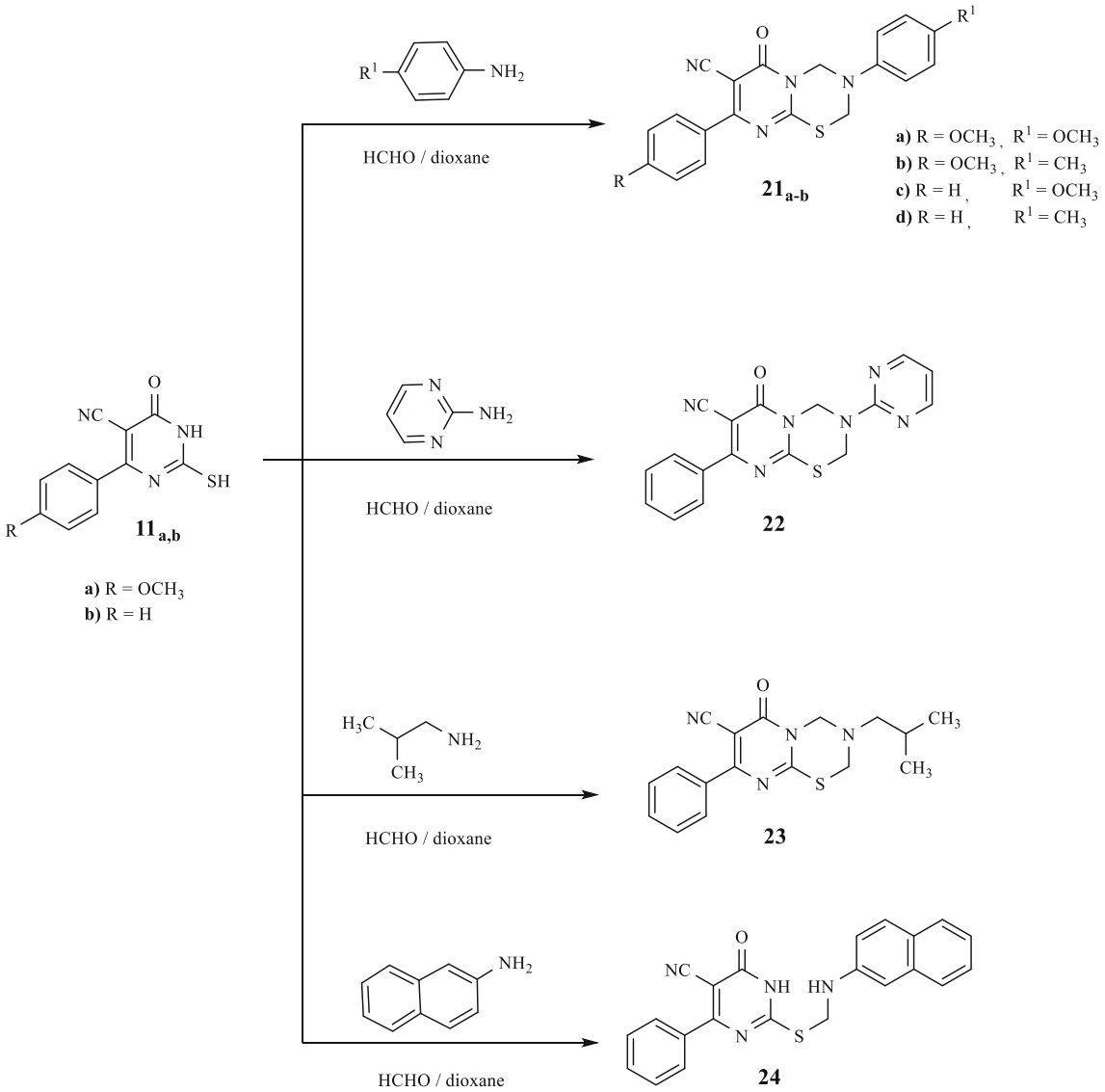

Scheme 4 General procedure for synthesis of target compounds $\mathbf{21_{a–d}}$–**24**

stabilized by a hydrogen bonding interaction with carbonyl backbone of Ala312, besides forming a water-mediated interaction with Asn112. Furthermore, the NH group at the 3-position formed a hydrogen bond with Asp218. The phenyl ring was stabilized by hydrophobic interactions with Met311, Leu221, Ile108 and aromatic stacking interaction with Trp109 and Phe225 (Fig. 5).

Overall, it was found that most of the studied compounds are expected to have the same binding mode of 5-FU and LYA. The designed molecules showed binding energies ranging from −37.24 to −83.71 kcal/mol (Table 2).

The proposed binding mode of compound **24** showed an affinity value of −83.71 kcal/mol engaging in several interactions with the protein. The bicyclic moiety was involved in aromatic stacking interactions with Phe80 and Phe225. Moreover, the bicyclic moiety was located in the hydrophobic pocket formed by Ile108 and Leu221. The phenyl ring was bonded by cationic–π interactions with Arg50 and Tyr258. The carbonyl group at the 6-position of pyrimidine moiety was anchored by hydrogen bonding interactions with Gln214 and Asn226. The cyano group at the 5-position of pyrimidine moiety is expected to participate in a hydrogen bonding interaction with Ser216. Due to the presence of extra hydrogen bonding and favorable interactions, compound **24** is predicted to have higher affinity toward the receptor compared over other compounds (Fig. 6).

On the other hand, compound $\mathbf{17_b}$ exhibited promising TS inhibitory activity (IC_{50} = 5.13 ± 0.11 μM and TS inhibition% = 79.28). Docking energy data of the compound $\mathbf{17_b}$ indicated that the ethyl acetate moiety is important for increasing the affinity toward the active site. Moreover, it was found that the binding mode of compound $\mathbf{17_b}$ is predicted

Table 1 In vitro anti-proliferative activities toward HePG-2, MCF-7, HCT-116 and PC-3 cell lines and thymidylate synthase (TS)

Comp.	IC_{50} (μM)[a]				TS	
	HePG-2	MCF-7	HCT-116	PC-3	IC_{50} (μM)[a]	Inhibition %
12	35.2 ± 0.72	28.4 ± 0.59	43.7 ± 0.69	42.2 ± 0.92	NT[c]	NT[c]
13	27.5 ± 0.33	16.5 ± 0.31	15.8 ± 0.26	13.1 ± 0.27	14.04 ± 0.63	49.37
14	35.4 ± 0.45	NA[b]	46.2 ± 0.83	NA[b]	NT[c]	NT[c]
15_a	30.9 ± 0.52	46.1 ± 1.06	NA[b]	38.9 ± 0.73	NT[c]	NT[c]
15_b	NA[b]	NA[b]	14.8 ± 0.32	NA[b]	NT[c]	NT[c]
16	38.8 ± 0.65	48.2 ± 0.77	36.7 ± 0.73	57.9 ± 1.27	NT[c]	NT[c]
17_a	25.5 ± 0.04	16.3 ± 0.34	19.2 ± 0.34	18.9 ± 0.35	5.49 ± 0.29	68.10
17_b	16.8 ± 0.03	8.7 ± 0.16	16.1 ± 0.30	10.6 ± 0.19	5.13 ± 0.11	79.28
18	NA[b]	NA[b]	NA[b]	NA[b]	NT[c]	NT[c]
19	29.2 ± 0.61	29.0 ± 049	28.2 ± 0.53	35.6 ± 0.60	NT[c]	NT[c]
20_a	NA[b]	NA[b]	45.1 ± 0.19	NA[b]	NT[c]	NT[c]
20_b	NA[b]	48.3 ± 0.33	NA[b]	NA[b]	NT[c]	NT[c]
21_a	28.6 ± 0.84	15.4 ± 0.33	28.5 ± 0.48	19.5 ± 0.73	5.3 ± 0.41	57.09
21_b	24.2 ± 0.53	9.7 ± 0.17	10.9 ± 0.20	27.3 ± 0.49	3.66 ± 0.44	70.41
21_c	11.1 ± 0.21	8.1 ± 0.13	10.00 ± 0.23	7.4 ± 0.15	2.14 ± 0.22	66.71
21_d	10.8 ± 0.22	13.8 ± 0.20	9.8 ± 0.15	11.9 ± 0.39	1.57 ± 0.08	83.09
22	16.8 ± 0.34	14.4 ± 0.34	17.2 ± 0.34	13.8 ± 0.27	3.51 ± 0.24	75.97
23	13.9 ± 0.25	16.6 ± 0.38	19.8 ± 0.35	15.0 ± 0.25	2.5 ± 0.65	81.43
24	6.4 ± 0.14	5.9 ± 0.11	7.9 ± 0.14	5.2 ± 0.09	3.89 ± 0.42	76.93
5-FU	8.5 ± 0.13	7.6 ± 0.15	9.3 ± 0.19	10.3 ± 0.18	1.84 ± 0.014	73.40

[a] IC_{50} values are the mean ± S.D. of three separate experiments
[b] NA: compounds with IC_{50} values >50 μM
[c] *NT* not tested

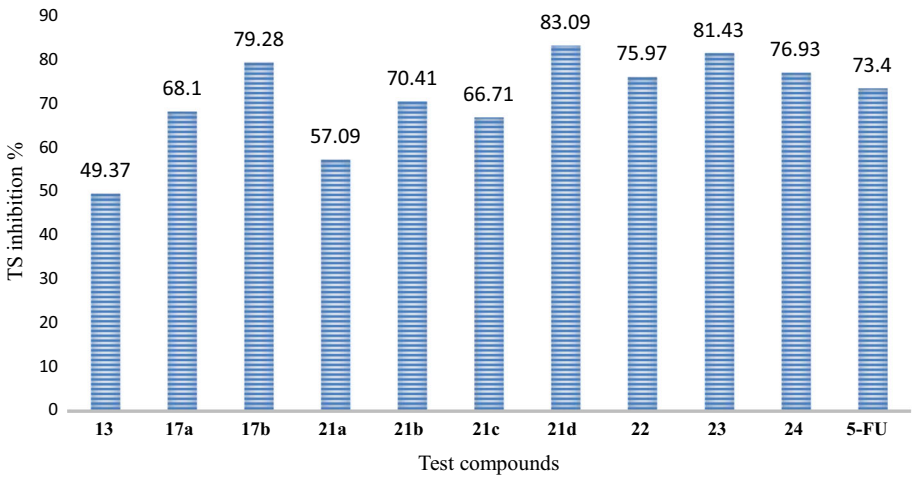

Fig. 3 TS inhibition % of test compounds and 5-FU (reference)

to be the same as that of compound **24**. In addition, the ethyl group of the compound **17_b** is stabilized by hydrophobic interactions with Ile108, Leu221 and Phe225. However, the substitution with carbonyl group can decrease the affinity for the receptor, where the carbonyl groups are surrounded by unfavorable interactions with nonpolar groups (Ile108 and Met311) (Fig. 7).

Compound **21_d** showed binding mode with TS similar to the general pattern observed by compound **24**. The hydrogen bonding interactions and aromatic stacking interactions were maintained. Compound **24** and **21_d** can fit nicely inside the binding pocket (Fig. 8).

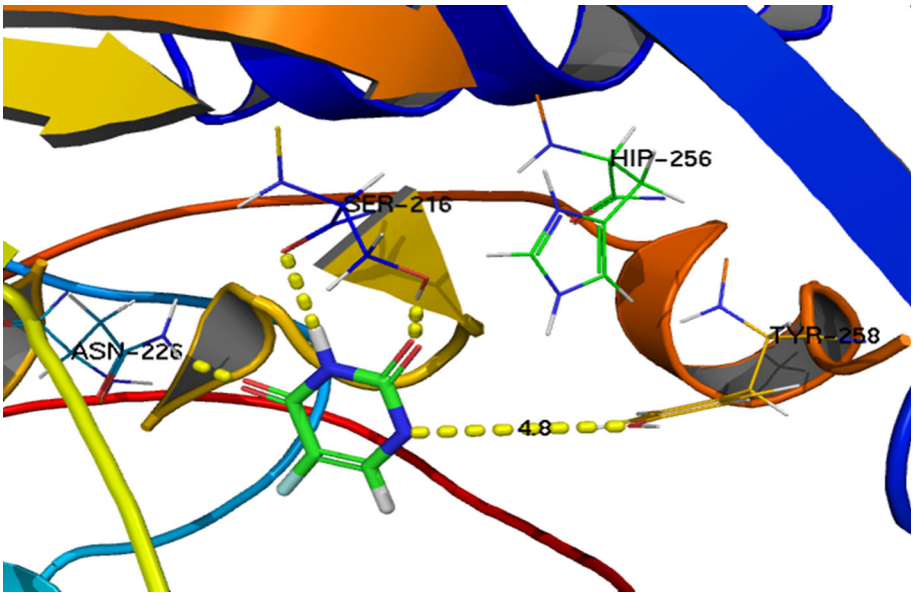

Fig. 4 Predicted binding mode of 5-FU at the TS binding site. H-bonds (*yellow dotted lines*), hydrogen atom (*gray*), nitrogen atom (*blue*), and oxygen atom (*red*). (Color figure online)

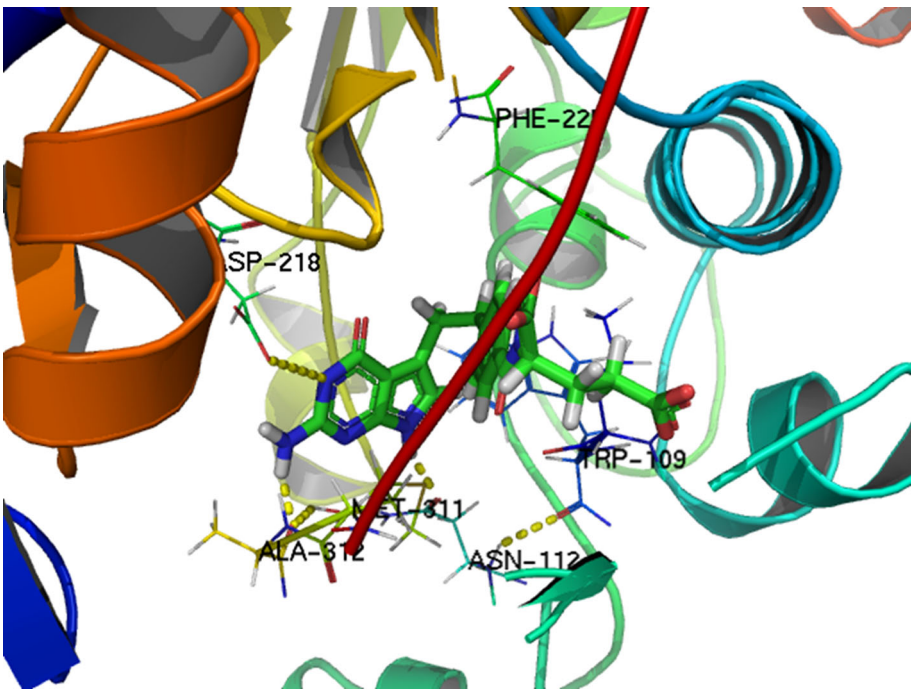

Fig. 5 Predicted binding mode of co-crystallized ligand (LYA) at the TS binding site. H-bonds (*yellow dotted lines*), hydrogen atom (*gray*), nitrogen atom (*blue*), and oxygen atom (*red*). (Color figure online)

Structure–activity relationships (SAR)

As outlined earlier, we first explored the effect of the chemical substitutions on the SH group with different alkyl and aralkyl moieties. The decreased IC_{50} values of compound **24** with naphthyl substitution at the SH group than those of their corresponding members **15**$_a$, **15**$_b$, **16**, **17**$_a$, **17**$_b$, **18** and **19** with alkyl substitutions indicated that substitution with aromatic moieties is advantageous.

With regard to the effect of substituting both the N-3 heteroatom and SH group with different alkyl and aralkyl moieties, it was found that the introduction two benzyl moieties (**20**$_a$ and **20**$_b$) resulted in a remarkable decrease in anti-proliferative activity in comparison with monosubstitutions (**15a**, **16**, **17**$_a$, **17**$_b$ and **19**).

The incorporation of a six-membered ring (**21**$_{a–d}$, **22** and **23**) was found to improve biologically versus the incorporation of a five-membered ring (**12**, **13**). Moreover, introduction of substituted aromatic or branched aliphatic moieties at the formed six-membered ring resulted in an increase in anti-proliferative activity.

Table 2 Docking binding free energies against TS

Comp.	ΔG kcal/mol	No. of hydrogen bonds	No. of cationic–π interactions
12	−48.61	1 (Asn112)	1 (Phe225)
13	−51.99	3 (His256, Ser216 and Asn226)	2 (Trp109 and Phe225)
14	−48.61	4 (Asn226, Asp218, Tyr258 and Arg50)	2 (Phe225 and Tyr258)
15_a	−45.85	1 (Tyr135)	2 (Trp109 and Tyr258)
15_b	−45.20	1 (Tyr135)	2 (Trp109 and Tyr258)
16	−44.85	3 (Asn226, Ser216 and Arg215)	2 (Phe225 and Tyr258)
17_a	−58.16	4 (Gln214, Asn226, His256 and Ser216)	3 (Tyr258, Phe225 and Trp109)
17_b	−63.60	3 (Gln214, Asn226 and Ser216)	3 (Ile108 and Met311, Tyr258 and Phe225)
18	−38.26	1 (Lys308)	1 (Phe225)
19	−45.85	3 (Ser216, His256 and Arg50)	3 (Phe225, Tyr258 and Trp109)
20_a	−40.20	0	2 (Phe225 and Tyr258)
20_b	−37.24	0	2 (Phe225 and Tyr258)
21_a	−57.22	2 (Ser216 and Asp218)	3 (Tyr258, Trp109 and Phe225)
21_b	−50.22	0	3 (Tyr258, Trp109 and Phe225)
21_c	−62.40	2 (Ser216 and Asp218)	3 (Tyr258, Trp109 and Phe225)
21_d	−63.06	2 (Ser216 and Asp218)	3 (Tyr258, Trp109 and Phe225)
22	−52.22	0	3 (Tyr258, Trp109 and Phe225)
23	−58.92	2 (Ser216 and Asp218)	2 (Trp109 and Tyr258)
24	−83.71	4 (Glu87, Asp218, Gln214 and Asn226)	6 (Phe225, Trp109, Tyr258, Met311, Ile108 and Leu221)
5-FU	−60.20	3 (Asn226 and Ser216)	2 (Phe225 and Leu221)
LYA	−90.32	3 (Ala312, Asn112 and Asp218)	6 (Met311, Ile108, Trp109, Phe225, Leu221 and Ile108)

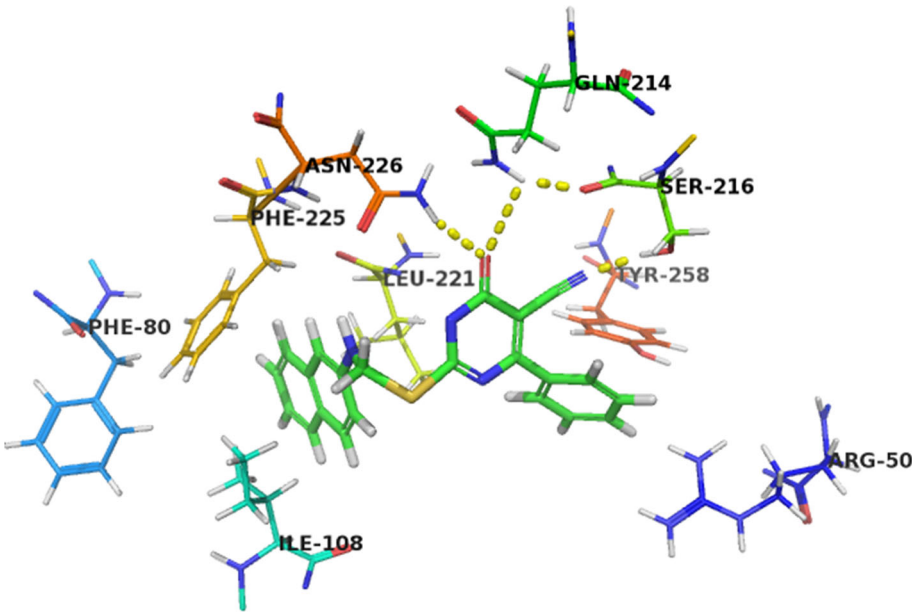

Fig. 6 Predicted binding mode of compound **24** at the binding site of TS. H-bonds (*yellow dotted lines*), hydrogen atom (*gray*), nitrogen atom (*blue*), oxygen atom (*red*) and sulfur atom (*yellow*). (Color figure online)

Conclusion

A series of 6-aryl-5-cyano thiouracil-based derivatives was designed, synthesized and evaluated for their in vitro anti-proliferative activities against HePG-2, MCF-7, HCT-116 and PC-3 cell lines as well as their TS inhibitory activities. Compounds **21_c**, **21_d** and **24** were the most potent anti-cancer members with IC_{50} values between 1.57 ± 0.08 and $11.9 \pm 0.39\,\mu M$ toward the tested cell lines. Interestingly, in vitro results of TS activity assay matched with the cytotoxicity trend of the compounds. Compounds **17_b**, **21_b**, **21_d**, **22**, **23** and **24** have demonstrated potent inhibitions more than 70%

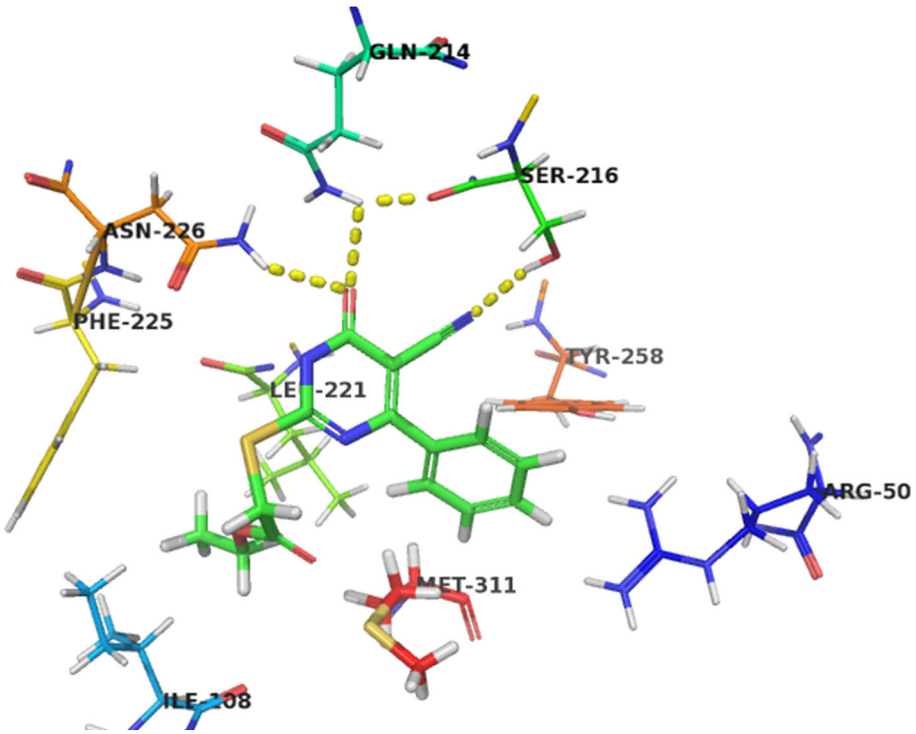

Fig. 7 Predicted binding mode for compound $\mathbf{17_b}$ at the binding site of TS. Carbonyl group is surrounded by unfavorable interactions with Ile108 and Met311

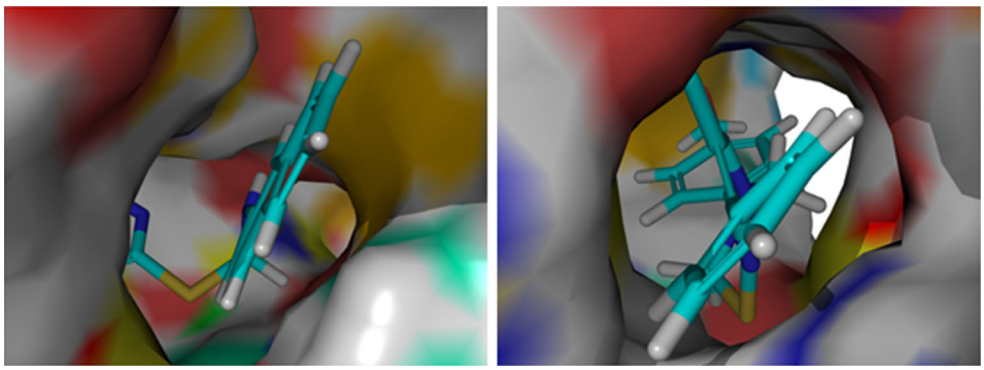

Fig. 8 3D predicted binding mode analysis for compounds **24** (*left*) and $\mathbf{21_d}$ (*right*) at the TS binding site

for the TS activity with IC_{50} values between 1.57 ± 0.08 and $5.13 \pm 0.11\,\mu M$. Docking studies also confirmed the results obtained from the in vitro thymidylate synthase (TS) assay and anti-proliferation test.

Materials and methods

Chemistry

General

Melting points were measured using a Gallenkamp melting point apparatus and were uncorrected. A Pye-Unicam SP-3-300 infrared spectrophotometer was used to record infrared (IR) spectra using KBr disks, and the data were expressed in wave number (cm^{-1}). ^1H NMR spectra were carried out at 400 and 300 MHz on BrukerAvance III and a Varian Mercury VX-300 NMR spectrometers, respectively; ^{13}C NMR spectra were run at 100 and 75 MHz. TMS was used as internal standard in deuterated dimethyl sulfoxide (DMSO-*d*6). Chemical shifts (δ) are expressed in ppm. A Shimadzu GCMS-QP-1000EX mass spectrometer was used to record mass spectra at 70 eV. A CHNO Rapid Analyzer was used to carry out elemental analyses (all compounds were within ± 0.4 of the theoretical values). TLC sheets coated with UV fluorescent silica gel Merck 60 F254 plates were used to carry out thin-layer chromatography to monitor the reactions. Compounds $\mathbf{11_{a,b}}$ are previously reported [33].

General procedure for synthesis of compounds (12–14)

A mixture of compounds **11$_{a,b}$** (0.01 mol), anhydrous K_2CO_3 (2.7 g, 0.02 mol) and tetrabutylammonium bromide (TBAB) (0.003 mol) in dry THF (50 mL) was stirred for 30 min at 80–82 °C. Then, appropriate dihalides, namely 2-dibromoethane, acetyl chloride and methylene chloride (0.012 mol), were added. The reaction mixture was stirred vigorously at room temperature for 8 h and monitoring by TLC. At end of the reaction, the reaction mixture was filtered, the filtrate evaporated, and the resulting residue washed three times using excessive amount of petroleum ether and then crystallized to produce the corresponding target compounds **12–14**, respectively.

7-(4-Methoxyphenyl)-5-oxo-2,3-dihydro-5H-thiazolo[3,2-a]pyrimidine-6-carbonitrile (12) White crystals (yield 77%); m.p. 245–247 °C (EtOH); IR (ν cm^{-1}) 3074 (CH-aromatic), 2999, 2971 (CH-aliphatic), 2212 (CN), 1663 (C=O);^{1}H NMR (300 MHz, DMSO-*d*6) δ (ppm): 3.62 (t, 2H, SCH_2, J = 8 Hz), 3.80 (s, 3H, OCH_3), 4.45 (t, 2H, NCH_2, J = 8 Hz), 7.10 (d, 2H, J = 8.8 Hz, H-3 and H-5 of phenyl), 7.90 (d, 2H, J = 9.8 Hz,Ar-H, H-2 and H-6 of phenyl);^{13}C NMR (75 MHz, DMSO-*d*6): 28.88, 49.91, 53.44, 92.83, 113.83, 115.80, 116.72, 126.52, 126.93, 129.52, 159.14, 159.63, 165.73, 172.46; MS (m/z): 287 (M^+ + 2, 10%), 255 (30%) 225 (100%); Anal. Calcd for $C_{14}H_{11}N_3O_2S$ (285.32): C, 58.94; H, 3.89; N, 14.73; Found: C, 58.69; H, 3.68; N, 14.63%.

2,5-Dioxo-7-phenyl-2,3-dihydro-5H-thiazolo[3,2-a]pyrimidine-6-carbonitrile (13) White crystals (yield 72%); m.p. 238–240 °C (EtOH); IR (ν cm^{-1}) br 3308 (OH), 3028 (CH-aromatic), 2998, 2941 (CH-aliphatic), 2227 (CN), 1716 (CO), 1652 (C=O amide); ^{1}H NMR (300 MHz, DMSO-*d*6) δ (ppm): 4.02 (s, 2H, CH_2), 7.64 (t, 2H, J = 6.9 Hz, Ar-H, H-3 and H-5 of phenyl), 7.94 (d, 2H, J = 6.9 Hz, Ar-H, H-2 and H-6 of phenyl); ^{13}C NMR (75 MHz, DMSO-*d*6): 93.43, 116.23, 129.76, 129.76, 129.00, 129.24, 129.24, 132.34, 135.49, 161.49, 165.89, 167.49, 169.64; MS (m/z) 271 (M^+ + 2, 5 %), 269 (M^+, 34%), 229 (47%), 104 (100%), 77 (62 %), 51 (38%); Anal. Calcd for $C_{13}H_7N_3O_2S$ (269.00): C, 57.99; H, 2.62; N, 15.61; Found: C, 57.68; H, 2.49; N, 15.51%.

2,2'-[Methylenebis(sulfanediyl)]bis[4-(4-methoxyphenyl)-6-oxo-1,6-dihydro pyrimidine-5-carbonitrile] (14) White powder (yield 78%); m.p. 293–295 °C (EtOH); IR (ν cm^{-1}) br 3161 (NH), 3107 (CH-aromatic), 2934, 2892 (CH-aliphatic), 2225 (CN), 1705 (C=O); ^{1}H NMR (400 MHz, DMSO-*d*6) δ (ppm): 2.73 (s, 1H, SCH), 2.88 (s, 1H, SCH), 3.80 (s, 3H, OCH_3), 7.11 (d, 4H, J = 8.8 Hz, Ar-H, H-3 and H-5 of phenyl), 7.65 (d, 4H, J = 8.8 Hz, H-2 and H-6 of phenyl), 13.07 (s, 2H, 2NH); ^{13}C NMR (100 MHz, DMSO-*d*6): 18.42, 55.33 (2), 95.42 (2), 115.91 (4), 120.96 (2), 130.34 (4), 133.53 (2), 158.57 (2), 163.48 (2), 167.81 (2), 170.14 (2); MS (m/z): 389 (2.5%), 273 (3 %) 259 (64%) 134 (100%), 91 (54%); Anal. Calcd for $C_{25}H_{18}N_6O_4S_2$ (530.58): C, 56.59; H, 3.42; N, 15.84; Found: C, 56.23; H, 3.30; N, 15.73%.

General procedure for synthesis of compounds (15–20)

A mixture of compounds **11$_{a,b}$** (0.01 mol), anhydrous K_2CO_3 (2.7g, 0.02 mol) and tetrabutylammonium bromide (TBAB) (0.003 mol) in dry THF (50 mL) was stirred for 30 min at 80–82 °C. Then, appropriate alkyl halide derivative, namely allyl bromide, ethyl chloroacetate, chloroacetic acid, diethyl bromomalonate, ethyl chloroformate and benzyl chloride (0.012 mol), was added. The reaction mixture was stirred vigorously at room temperature for 4 h and monitored by TLC. After completion of the reaction, the reaction mixture was filtered, the filtrate evaporated, and the resulting residue washed three times using excessive amount of petroleum ether and then crystallized to produce the corresponding target compounds **15–20**, respectively.

2-(Allylthio)-4-(4-methoxyphenyl)-6-oxo-1,6-dihydropyrimidine-5-carbonitrile (15$_a$) Yellowish crystals (yield 81%); m.p. 251–253 °C (EtOH); IR(ν cm^{-1}) 3200 (NH), 3072 (CH-aromatic), 2934, 2838 (CH-aliphatic), 2216 (CN), 1651 (C=O)amid; ^{1}H NMR (400 MHz, DMSO-*d*6) δ (ppm): 3.85 (s, 3H, OCH_3), 3.94 (d, 2H, SCH_2, J = 6.8 Hz), 5.15 (s, 2H, $C\underline{H}_2$ = CH, J = 5.6 Hz), 5.95 (q, 1H, CH=, J = 7 Hz), 7.13 (d, 2H, J = 7.2 Hz, Ar-H, Ar-H, H-3 and H-5 of phenyl), 8.02 (d, 2H,, J = 7.2 Hz, Ar-H, H-2 and H-6 of phenyl), 13.65 (s, 1H, NH, D_2O exchangeable); ^{13}C NMR (75 MHz, DMSO-*d*6): 13.21, 20.32, 55.44, 61.35, 91.24, 114.27, 114.5, 127.53, 127.92, 132.44, 159.45, 162.44, 168.93, 169.90, 170.68; MS (m/z): 331 (M^+ +2, 35%), 299 (M^+ +2, 15%), 258 (100%); Anal. Calcd for $C_{15}H_{13}N_3O_2S$ (299.35): C, 60.19; H, 4.38; N, 14.04; Found: C, 59.89; H, 4.18; N, 13.98%.

2-(Allylthio)-6-oxo-4-phenyl-1,6-dihydropyrimidine-5-carbonitrile (15$_b$) Yellowish crystals (yield 83%); m.p. 238–240 °C (EtOH); IR(ν cm^{-1}) 3435 (NH), 3018 (CH-aromatic), 2937, 2856 (CH-aliphatic), 2219 (CN), 1654 (C=O); ^{1}H NMR (400 MHz, DMSO-*d*6) δ (ppm): 3.90 (d, 2H, SCH_2, J = 6.8 Hz), 5.31 (d, 2H, $C\underline{H}_2$ = CH, J = 5.6 Hz), 5.92 (q, 1H, CH=, J = 7 Hz), 7.45 (d.d, 1H, J = 8.1 Hz, Ar-H, H-4 of phenyl), 7.58 (t, 2H, J = 7.5 Hz, Ar-H, H-3 and H-5 of phenyl), 7.94 (d, 2H, J = 7.5 Hz, Ar-H, H-2 and H-6 of phenyl); ^{13}C NMR (100 MHz, DMSO-*d*6): 14.33, 30.24, 62.34, 95.36, 115.13, 126.32, 126.91, 128.21, 128.18, 128.87, 139.25, 161.92, 167.44, 170.45; MS (m/z): 271 (M^+ + 2, 45%), 269 (M^+, 28%), 228 (100 %); Anal. Calcd for $C_{14}H_{11}N_3OS$ (269.32): C, 62.44; H, 4.12; N, 15.60; Found: C, 62.15; H, 4.0; N, 15.49%.

2-{[5-Cyano-4-(4-methoxyphenyl)-6-oxo-1,6-dihydropyrimidin-2-yl]thio} acetic acid (16) White powder (yield 75%); m.p. 233–235 °C (EtOH); IR (ν cm^{-1}) 2750–3514 (br OH-carboxylic), 3200 (NH), 3009 (CH-aromatic), 2933, 2842 (CH-aliphatic), 2219 (CN), 1717 (C=O carboxylic) acid, 1651 (C=O); ^{1}H NMR (400 MHz, DMSO-*d*6) δ (ppm): 3.86 (s, 3H, OCH_3), 4.06 (s, 2H, SCH_2), 7.10 (d, 2H, J = 8 Hz, Ar-H, H-3 and H-5 of phenyl), 8.01 (d, 2H, J = 8 Hz, Ar-H, H-2 and H-6 of phenyl), 13.17 (s, 1H, NH, D_2O exchangeable), 13.23 (s, 1H, OH, D_2O exchangeable); ^{13}C NMR (100 MHz, DMSO-*d*6): 18.92, 33.52, 56.01, 56.42, 91.74, 114.45, 116.73, 127.52, 131.41, 161.58, 162.71, 165.28, 166.58, 169.67; MS (m/z) 317 (M^+, 3.1 %), 298 (100%); Anal. Calcd for $C_{14}H_{11}N_3O_4S$ (317.29): C, 52.99; H, 3.49; N, 13.24; Found: C, 52.79; H, 3.31; N, 13.15%.

Ethyl 2-((5-cyano-4-(4-methoxyphenyl)-6-oxo-1,6-dihydropyrimidin-2-yl) thio)acetate (17$_a$) Gray powder (yield 78%); m.p. 212–214 °C (EtOH); IR (ν cm^{-1}) 3301 (NH), 3013 (CH-aromatic), 2982 (CH-aliphatic), 2218 (CN), 1737 (CO ester), 1655 (C=O amide); ^{1}H NMR (400 MHz, DMSO-*d*6) δ (ppm): 1.23 (t, 3H, CH_3, J = 7.2 Hz), 3.86 (s, 2H, SCH_2), 4.01 (s, 3H, OCH_3), 4.07 (q, 2H, OCH_2, J = 6 Hz), 7.16 (d, 2H, J = 8.7 Hz, Ar-H, H-3 and H-5 of phenyl), 8.04 (d, 2H, J = 8.7 Hz, Ar-H, H-2 and H-6 of phenyl) 13.8 (s, 1H, NH, D_2O exchangeable); ^{13}C NMR (100 MHz, DMSO-*d*6): 14.38, 33.35, 56.03, 61.77, 91.87, 114.43, 115.36, 116.63, 127.42, 131.31, 133.70, 162.81, 164.93, 166.4, 168.48, 169.69; MS (m/z): 347 (M^+ + 2, 18%), 300 (33%), 258 (75%), 122 (100%); Anal. Calcd for $C_{16}H_{15}N_3O_4S$: (345.37): C, 55.64; H, 4.38; N, 12.17; Found: C, 55.37; H, 4.19; N, 12.05%.

Ethyl2-[(5-cyano-6-oxo-4-phenyl-1,6-dihydropyrimidin-2-yl]thio)acetate (17$_b$) White crystal (yield 75%); m.p. 240–242 °C (EtOH); IR(ν cm^{-1}) 3203 (NH), 3013 (CH-aromatic), 2985, 2941 (CH-aliphatic), 2222 (CN), 1735 (C=O ester), 1660 (CO amide); ^{1}H NMR (400 MHz, DMSO-*d*6) δ (ppm): 1.09 (t, 3H, CH_3, J = 7 Hz), 4.11 (s, 2H, SCH_2), 4.05 (q, 2H, OCH_2, J = 7.2 Hz), 7.58 (dd, 1H, J = 6.9 Hz, Ar-H, H-4 of phenyl), 7.74 (t, 2H, J = 7.8 Hz, Ar-H, H-3 and H-5 of phenyl), 7.90 (d, 2H, J = 7.8 Hz, Ar-H, H-2 and H-6 of phenyl); ^{13}C NMR (100 MHz, DMSO-*d*6): 14.80, 15.92, 59.83, 94.32, 116.31, 126.22, 126.86, 128.15, 128.38, 128.79, 137.39, 159.93, 166.36, 169.35, 170.88; MS (m/z): 315 [M^+, 12 %), 269 (11%), 242 (27%), 104 (26%), 91(100%); Anal. Calcd for $C_{15}H_{13}N_3O_3S$: (315.35): C, 57.13; H, 4.16; N, 13.33; Found: C, 56.95; H, 3.99; N, 13.21%.

Diethyl2-{[5-cyano-4-(4-methoxyphenyl)-6-oxo-1,6-dihydropyrimidin-2-l] thio}vmalonate (18) White crystal (yield 77%); m.p. 214–216 °C (EtOH IR (ν cm^{-1}) 3205 (NH), 3055 (CH-aromatic), 2992, 2942 (CH-aliphatic), 2226 (CN), 1705 (C=O ester), 1645 (C=O amide); ^{1}H NMR (400 MHz, DMSO-*d*6) δ (ppm): 1.20 (t, 6H, $2CH_3$, J = 7.2 Hz), 3.88 (s, 3H, OCH_3), 4.02 (q, 4H, $2CH_2$, J = 7.2 Hz), 5.01 (s, 1H, SCH), 7.25 (d, 2H, J = 9.6 Hz, Ar-H, H-3 and H-5 of phenyl), 7.96 (d, 2H, J = 8.8 Hz, Ar-H, H-2 and H-6 of phenyl), 12.50 (s, 1H, NH, D_2O exchangeable); ^{13}C NMR (100 MHz, DMSO − *d*6): 14.32, 14.24, 45.33, 55.32, 93.17, 114.64, 114.78, 127.46 (2), 127.94 (2), 160.51 (2), 160.96 (2), 164.35, 174.37, 166.76, 170.85; MS (m/z): 419 (M^+ + 2, 77%), 259 (100%),; Anal. Calcd for $C_{19}H_{19}N_3O_6S$: (417.44): C, 54.67; H, 4.59; N, 10.07; Found; C, 54.39; H, 4.45; N, 9.97%.

S-[5-Cyano-4-(4-methoxyphenyl)-6-oxo-1,6-dihydropyrimidin-2-yl]propane thioate (19) Yellow crystal (yield 79%); m.p. 216–218 °C (EtOH); IR (ν cm^{-1}) 3151 (NH), 3078 (CH-aromatic), 2996, 2939 (CH-aliphatic), 2239 (CN), 1785 (C=O ester), 1701 (C=O amide); ^{1}H NMR (400 MHz, DMSO-*d*6) δ (ppm): 1.04 (t, 3H, CH_3, J = 7.2 Hz), 3.85 (s, 3H, OCH_3), 4.23 (q, 2H, CH_2, J = 7.2 Hz), 7.25 (d, 2H, J = 8.8 Hz, Ar-H, H-3 and H-5 of phenyl), 7.96 (d, 2H, Ar-H, J = 8.8 Hz, Ar-H, H-2 and H-6 of phenyl), 12.50 (s, 1H, NH, D_2O exchangeable); ^{13}C NMR (100 MHz, DMSO-*d*6): 14.72, 55.67, 62.79, 93.70, 114.68, 114.85, 115.65, 127.45, 127.93, 129.89, 158.25, 159.41, 159.97, 166.67, 170.78; MS (m/z): 389 (M^+, 2.5%), 273 (3%) 259 (64%) 134 (100%); Anal. Calcd for $C_{15}H_{13}N_3O_3S$; (331.06): C, 54.37; H, 3.95; N, 12.68; Found C, 54.08; H, 3.83; N, 12.55%.

1-Benzyl-2-(benzylthio)-4-(4-methoxyphenyl)-6-oxo-1,6-dihydropyrimidine-5-carbonitrile (20a) Reddish crystals (yield 65%); m.p. 170–172 °C (EtOH); IR (ν cm^{-1}) 3060 (CH-aromatic), 2964, (CH-aliphatic), 2212 (CN), 1674 (C=O); 1H NMR (400 MHz, DMSO-*d*6) δ (ppm): 3.84 (s, 3H, CH_3O), 4.50, 4.59 (s, s, 2H, SCH_2), 5.2 and 5.6 (s, s, 2H, NCH_2), 7.13–8.05 (m, 14H, Ar-H); ^{13}C NMR (100 MHz, DMSO-*d*6): 35.18, 36.78, 47.96, 56.00, 69.93, 87.32, 91.42, 114.60, 114.65, 115.44, 116.71, 127.73, 128.51, 128.98, 129.56, 131.44, 134.57, 135.73, 137.63, 160.75, 162.71, 164.75, 166.14, 167.81, 169.55, 173.97; MS (m/z): 439 (M^+, 100 %), 330 (10%), 270 (12%), 211 (40%), 139 (62%), 56 (51%) . Anal. Calcd for $C_{26}H_{21}N_3O_2S$; (439.53): C, 71.05; H, 4.82; N, 9.56; Found: C, 70.75; H, 4.76; N, 9.45%.

2-(Benzylthio)-6-oxo-1,4-diphenyl-1,6-dihydropyrimidine-5-carbonitrile (20$_b$) White crystals (Yield 69%); m.p. 185–187 °C (EtOH); IR(ν cm^{-1}) 3078 (CH-aromatic), 2996, 2939(CH-aliphatic), 2212 (CN), 1674 (C=O); ^{1}HNMR (400 MHz, DMSO-*d*6) δ (ppm): 4.50 (s, 2H, NCH_2), 5.28 (s, 2H, SCH_2), 7.31–7.98 (m,15H, Ar-H); ^{13}C NMR (100 MHz, DMSO-*d*6): 137.64, 45.96, 94.23, 116.43, 126.46(2), 126.68, 126.93 (2), 127.21 (2), 127.61, 127.72 127.93 (2), 128.44 (2), 128.65, 128.92 (2), 136.44, 136.94, 160.28, 162.83, 170.58; MS (m/z): 409 (M^+, 1.17%), 318 (13 %), 148 (19%), 141

(33%), 139 (100%), 91 (53%); Anal. Calcd for $C_{25}H_{19}N_3OS$; (409.51): C, 73.33; H, 4.68; N, 10.26; Found: C, 73.06; H, 4.51; N, 10.16%.

General procedures for synthesis of compounds (21–24)

A mixture of compounds $\mathbf{11_{a,b}}$ (1.0 mmol), appropriate primary amines, namely *p*-anisidine, *p*-toluidine, 2-aminopyrimidine, iso-butylamine and β-naphthylamine (1.1 mmol), and formaldehyde (2 mL) was stirred in dioxane (40 mL) at room temperature for 3 h. The resulting precipitate was collected by filtration, washed with water several times and dried. The crude product was crystallized using a proper solvent to give the corresponding title compounds **21–24**, respectively.

3,8-Bis(4-methoxyphenyl)-6-oxo-3,4-dihydro-2H,6H-pyrimido[2,1-b][1,3,5] thiadiaine-7-carbonitrile (***21$_a$***) Pale yellow crystal (yield 91%); m.p. 225–228 °C (EtOH); IR (ν cm^{-1}) 3055 (CH-aromatic), 2994 (CH-aliphatic), 2214 (CN) 1645 (C=O); ^{1}H NMR (400 MHz, DMSO-*d*6) δ (ppm): 3.69(s, 3H, OCH_3), 3.83 (s, 3H, OCH_3), 5.46 (s, 2H, S–CH_2–N), 5.67 (s, 2H, N–CH_2-N), 6.92 (d, 2H, Ar-H, H-3 and H-5 of phenyl, J = 8 Hz), 7.08 (d, 2H, Ar-H, H-2 and H-6 of phenyl, J = 8 Hz), 7.10 (d, 2H, Ar-H, H-3 and H-5 of phenyl, J = 9.2 Hz), 7.90 (d, 2H, Ar-H, H-2 and H-6 of phenyl, J = 9.2 Hz); ^{13}C NMR (100 MHz, DMSO-*d*6): 55.23, 55.86, 70.27, 93.29, 114.26 (2), 115.24(2), 115.93 (2), 127.72 (2), 129.23, 142.25, 153.24, 159.28, 160.98, 163.29, 170.84; MS (m/z): 408 (M^+ + 2, 100%); Anal. Calcd for $C_{21}H_{18}N_4O_3S$; (406.46): C, 62.06; H, 4.46; N, 13.78; Found: C, 61.89; H, 4.29; N, 13.69%.

8-(4-Methoxyphenyl)-6-oxo-3-(p-tolyl)-3,4-dihydro-2H, 6H-pyrimido[2,1-b] [1,3,5] thiadiaine-7-carbonitrile (***21$_b$***) Yellowish powder (yield 88%); m.p. 228–230 °C (EtOH); IR (ν cm^{-1}) 3102 (CH-aromatic), 2915 (CH-aliphatic), 2219 (CN) 1658 (C=O); ^{1}H NMR (400 MHz, DMSO-*d*6) δ (ppm): 2.21 (s, 3H, CH_3), 3.83 (s, 3H,-OCH_3), 5.49 (s, 2H, S–CH_2–N), 5.71 (s, 2H, N–CH_2-N), 7.04 (d, 2H, Ar-H, H-2 and H-6 of P − tolyl, J = 6.8 Hz), 7.07 (d, 2H, Ar-H, H-3 and H-5 of *P*-methoxy phenyl, J = 8.4 Hz), 7.15 (d, 2H, Ar-H,H-3 and H-5 of *P*-tolyl, J = 6.8 Hz), 7.90 (d, 2H, Ar-H,H-2 and H-6 of *P*-methoxy phenyl, J = 8.4 Hz); ^{13}C NMR (100 MHz, DMSO-*d*6): 21.56, 55.64, 55.96, 70.52, 93.59, 112.44 (2), 114.33 (2), 115.41, 127.46 (2),129.15, 129.73(2), 130.73, 160.44, 162.42, 163.64, 170.75; MS (m/z): 392 (M^+ +2, 24%), 225 (100%); Anal. Calcd for $C_{21}H_{18}N_4O_2S$; (390.46): C, 64.60; H, 4.65; N, 14.35; Found: C, 64.39; H, 4.46; N, 14.29%.

3-(4-Methoxyphenyl)-6-oxo-8-phenyl-3,4-dihydro-2H,6H-pyrimido[2,1-b] [1,3,5] thiadiazine-7-carbonitrile (21c) Pale yellow crystals (yield 79%); m.p. 225–227 °C (EtOH / Benzene); IR(ν cm^{-1}) 3041(CH-aromatic), 2955 (CH-aliphatic), 2215 (CN), 1652 (C=O); ^{1}H NMR (300 MHz, DMSO-*d*6) δ: (ppm): 3.67 (s, 3H, OCH_3), 5.45 (s, 2H, S–CH_2–N), 5.76 (s, 2H, N–CH_2–N), 6.90 (d, 2H, Ar-H, H-3 and H-3 of *P*-methoxy phenyl, J = 8.2 Hz), 7.10 (d, 2H, Ar-H, H-2 and H-6 of *P*-methoxy phenyl, J = 8.2 Hz), 7.33 (dd, 1H, J = 7.00 Hz, Ar-H, H-4 of phenyl), 7.53 (t, 2H, J = 8.1 Hz, Ar-H, H-3 and H-5 of phenyl), 7.82 (d, 2H, J = 8.1 Hz, Ar-H, H-2 and H-6 of phenyl); ^{13}C NMR (75 MHz, DMSO-*d*6): 55.00, 55.66, 62.21, 92.30, 115.35, 115.99, 118.69, 129.01, 129.03, 132.28, 132.30, 134.97 134.99, 137.33, 137.34 137.35, 155.32, 153.63, 165.45, 166.27; MS (m/z): 378 (M^+ + 2, 55%), 229 (100%); Anal. Calcd for $C_{20}H_{16}N_4O_2S$: (376.43): C, 63.81; H, 4.28; N, 14.88; Found: C, 63.54; H, 4.17; N, 14.79%.

6-Oxo-8-phenyl-3-(p-tolyl)-3,4-dihydro-2H,6H-pyrimido[2,1-b][1,3,5]thiadiazine-7-carbonitrile (***21$_d$***) White crystals (yield 85%); m.p. 220–222 °C (EtOH, Benzene); IR (ν cm^{-1}) 3049 (CH-aromatic), 2915 (CH-aliphatic), 2214 (CN), 1653 (C=O); ^{1}H NMR (300 MHz, DMSO-*d*6) δ: (ppm): 2.25 (s, 3H, CH_3), 5.50 (s, 2H, S–CH_2–N), 5.73 (s, 2H, N–CH_2–N), 7.65 (d, 2H, Ar-H, H-2 and H-6 of *p*-tolyl), 7.16 (d, 2H, Ar-H, H-3 and H-5 of *p*-tolyl), 7.50 (dd, 1H, J = 7.4 Hz, Ar-H, H-4 of phenyl), 7.66 (t, 2H, J = 7.4 Hz, Ar-H, H-3 and H-5 of phenyl), 7.83 (d, 2H, J = 8.4 Hz, Ar-H, H-2 and H-6 of phenyl); ^{13}C NMR (75 MHz, DMSO-*d*6): 22.14, 55.46, 70.30, 94.20, 112.35 (2), 115.75, 126.37 (2), 127.14, 128.30(2), 129.26 (2), 130.66, 137.72, 147.87, 160.19, 163.75, 170.78; MS (m/z): 362 (M^+ + 2, 33%), 229 (100%); Anal. Calcd for $C_{20}H_{16}N_4OS$: (360.44) C, 66.65; H, 4.47; N, 15.54; Found: C, 66.37; H, 4.53; N, 4.41%.

6-Oxo-8-phenyl-3-(pyrimidin-2-yl)-3,4-dihydro-2H,6H-pyrimido[2,1-b] [1,3, 5] thiadiazine-7-carbonitrile (22) White crystals (yield 85%); m.p. 248–250 °C (EtOH); IR (ν cm^{-1}) 3059 (CH-aromatic), 2940 (CH-aliphatic), 2230 (CN), 1679 (C=O); ^{1}H NMR (300 MHz, DMSO-*d*6) δ: (ppm): 5.52 (s, 2H, S–CH_2–N), 5.77 (s, 2H, N–CH_2–N), 6.87–8.55 (m, 8H, Ar-H); MS (m/z): 348 (M^+, 45%), 229 (48%), 108 (100%); ^{13}C NMR (75 MHz, DMSO-*d*6): 55.64, 70.34, 94.25, 115.66, 115.89, 126.63(2), 127.55, 128.94(2), 135.34, 158.24(2), 160.34, 162.35, 162.96, 171.19; MS (m/z): 350 (M^+ + 2, 100%), 228 (22%) Anal. Calcd for $C_{17}H_{12}N_6OS$ (348.38) C, 58.61; H, 3.47; N, 24.12; Found: C, 58.29; H, 3.29; N, 24.04%.

3-Isobutyl-6-oxo-8-phenyl-3,4-dihydro-2H,6H-pyrimido[2,1-b][1,3,5]thiadiazine-7-carbonitrile (23) Pale yellow crystal (yield 82%); m.p. 218–220 °C (EtOH); IR (ν cm^{-1}) 3150 (CH-aromatic), 2954 (CH-aliphatic), 2215 (CN), 1670 (C=O); ^{1}H NMR (300 MHz, DMSO-*d*6) δ (ppm): 0.92 (d, 6H, 2CH_3, J = 5.7 Hz), 1.83 (m, H, CH, J = 7.2 Hz),

1.83 (d, 2H, CH_2, $J = 7.2$ Hz), 4.90 (s, 2H, S–CH_2–N), 5.09 (s, 2H, N–CH_2–N), 7.51 (dd, 1H, $J = 7.49$ Hz, Ar-H, H-4 of phenyl), 7.56 (t, 2H, $J = 8.2$ Hz, Ar-H, H-3 and H-5 of phenyl), 7.71 (d, 2H, $J = 8.2$ Hz, Ar-H, H-2 and H-6 of phenyl); ^{13}C NMR (75 MHz, DMSO-*d*6): 21.32(2), 25.38, 54.34, 62.45, 68.24, 93.93, 115.45, 126.75(2), 127.83, 128.94(2), 136.65, 160.35, 162.86, 170.70; MS (m/z): 326 (M^+, 95%), 293 (28%); Anal. Calcd for $C_{17}H_{18}N_4OS$; (326.42): C, 62.55; H, 5.56; N, 17.16; Found: C, 62.23; H, 5.45; N, 17.08%.

2-(((Naphthalen-2-ylamino)methyl)thio)-6-oxo-4-phenyl-1,6-dihydropyrimidine-5-carbonitrile (24) Reddish brown crystal (yield 77%), m.p. 165–167 °C (EtOH); IR(ν cm^{-1}) 3163 (NH), 3031 (CH-aromatic), 2852 (CH-aliphatic), 2221 (CN), 1671 (C=O); ^{1}H NMR (300 MHz, DMSO-*d*6) δ (ppm): 3.51 (s, 2H, CH_2), 7.21 (s, 1H, NH-naphthyl, D_2O exchangeable), 7.55–7.81 (m, 11H, Ar-H), 12.99 (s, 1H, NH pyrimidine, D_2O exchangeable); ^{13}C NMR (75 MHz, DMSO-*d*6): 45.83, 94.41, 105.52, 115.32, 118.64, 121.43, 121.83, 124.42, 125.44 (2), 126.46, 126.84, 127.14, 127.96 (2), 128.48, 136.46, 138.94, 144.83, 160.46, 167.35, 171.95; MS (m/z): 386 ($M^+ + 2$, 17%), 288 (100%); Anal. Calcd for $C_{22}H_{16}N_4OS$ (384.46): C, 68.73; H, 4.20; N, 14.57; Found: C, 68.51; H, 4.10; N, 14.44%.

Biological evaluation

In vitro anti-proliferative activity

Four human cancer cell lines, namely hepatocellular carcinoma (HePG-2), mammary gland (MCF-7), colorectal carcinoma (HCT-116) and human prostate cancer (PC-3), are used to determine in vitro the anti-proliferation properties of the synthesized compounds. The tested cell lines were supplied from the US National Cancer Institute. The reported standard procedure described by Skehan et al. [32] was utilized in this test as follows.

The tested cells were plated in 96-well microplates; the total volume per well was adjusted at 100 µL. Then, incubation of cells was performed at 37 °C, 5% CO_2, 95% air and 100% relative humidity for 24 h before addition of synthesized compounds. After 24 h, only two plates of each cell line were selected and fixed in situ with TCA, in order to exemplify a measurement of the cell population for each cell line during drug application. The title compounds and fluorouracil, the reference drug, were dissolved in DMSO at 400-fold the desired final maximum test concentration and stored at freezing point prior to use. During addition of drug, the frozen concentrate was dissolved and diluted to twice the desired final maximum test concentration with gentamicin solution (50 mg/mL). To reach the desired final drug concentrations, different tested compound dilutions (100 mL) were added to the appropriate microtiter wells containing 100 mL of medium. The tested compounds as well as 5-fluorouracil as reference drug were added. Then, the plates were incubated for an additional 48 h at 37 °C, 5% CO_2, 95% air and 100% relative humidity. The assay was terminated by addition of cold TCA for adherent cells followed by incubation for 60 min at 4 ° C. The supernatant was removed, and the plates were washed five times with excessive water and dried. A solution of 0.4% (w/v) sulforhodamine B (100 mL) in 1% acetic acid was added to each well, followed by incubation at room temperature for 10 min. After staining, the plates were washed with 1% acetic acid to remove unbound dye and air-dried. Bound stain was dissolved with 10 mM Trizma base. Spectrophotometric assay of the optical density (OD) of each well was determined at 564 nm with an ELISA microplate reader (ChroMate-4300, FL, USA). Boltzmann sigmoidal concentration response curve was used to calculate the IC_{50} values through the nonlinear regression fitting models (GraphPad Prism, version 5). The means of three separate experiments was reported as final result. ANOVA test was used to analyze the statistical differences, wherein the differences were considered to be significant at $p < 0.05$.

In vitro assay of thymidylate synthase (TS) activity

The kinase activity of TS was measured spectrophotometrically at pH 7.4 and 30 °C in a mixture containing 0.1 M 2-mercaptoethanol, 0.0003 M (6R,S)-tetrahydrofolate, 0.02 M $MgCl_2$, 0.012 M formaldehyde, 0.04 M TrisHCl, 0.001 M dUMP and 0.00075 M Na EDTA according to the reported procedure described by Wahba and Friedkin [37]. In general, to initiate the reaction, the enzyme was added in the absence of inhibitor producing a change in absorbance at 340 nm of 0.016/min. Then, four inhibitor concentrations were used to determine the percent inhibition. Next, concentration–inhibition response curve for the test compounds was generated to determine median inhibitory concentration (IC_{50}). The obtained data were compared with 5-fluorouracil as a standard TS inhibitor. The standard deviations for determination of the 50% points were within ±10% of the values given.

Molecular docking

All docking studies were performed using AutoDock 4.2 program [38,39]. The structure of the synthesized compounds and reference ligands was drawn using ACD/ChemSketch (version 12.0, Toronto, Canada) [40], and their geometry was optimized by Autodock 4.2. The scoring function used is empirically derived for empirical binding free energy force field that allows the prediction of binding free energies for docked ligands. The 3D crystal structure of the thymidylate

synthase (TS) was downloaded from the Brookhaven Protein Databank (PDB ID: 1JU6, 2.89 Å resolution) [41]. All bound waters ligands and cofactors were removed from the protein prior to the docking process. Then, SPDBV-Swiss-pdb viewer [42] was used to minimize the energy. Next, hydrogen atoms were added for the minimized receptor. Kollman charges and solvation parameters were applied. In order to include all the amino acid residues, the precalculated grid maps are set at the size of 60, 60 and 60 Å (x, y and z). The spacing between grid points was 0.575 Å. The Lamarckian genetic algorithm (LGA) was utilized in the docking process. All the test compounds were docked within the prepared grid. The crystallized pose of 5-fluorouracil and pemetrexed (LYA) was used as standards. The output from AutoDock was further analyzed with PyMOL software package [43].

Acknowledgements Authors are thankful to the scientific research team of VASERA CO., Giza, Egypt, for providing laboratory facilities for biological activity.

Compliance with ethical standards

Conflict of interest This work was funded by the authors, and there is no any conflict of interest.

References

1. Jemal A, Murray T, Ward E, Samuels A, Tiwari RC, Ghafoor A, Feuer EJ, Thun MJ (2005) Cancer statistics, 2005. CA Cancer J Clin 55:10–30. doi:10.3322/canjclin.55.1.10
2. Hanahan D, Weinberg RA (2011) Hallmarks of cancer: the next generation. Cell 144:646–674. doi:10.1016/j.cell.2011.02.013
3. Siegel RL, Miller KD, Jemal A (2016) Cancer statistics, 2016. CA Cancer J Clin 66:7–30. doi:10.3322/caac.21332
4. Eissa IH, El-Naggar AM, El-Hashash MA (2016) Design, synthesis, molecular modeling and biological evaluation of novel 1H-pyrazolo[3,4-b]pyridine derivatives as potential anticancer agents. Bioorg Chem 67:43–56. doi:10.1016/j.bioorg.2016.05.006
5. WHO. Cancer. http://www.who.int/cancer/en/. Access 22 May 2016
6. Costi MP, Tondi D, Rinaldi M, Barlocco D, Pecorari P, Soragni F, Venturelli A, Stroud RM (2002) Structure-based studies on species-specific inhibition of thymidylate synthase. Biochim Biophys Acta 1587:206–214. doi:10.1016/S0925-4439(02)00083-2
7. Carreras CW, Santi DV (1995) The catalytic mechanism and structure of thymidylate synthase. Annu Rev Biochem 64:721–762. doi:10.1146/annurev.bi.64.070195.003445
8. Backus H, Wouters D, Ferreira C, Van Houten V, Brakenhoff R, Pinedo H, Peters G (2003) Thymidylate synthase inhibition triggers apoptosis via caspases-8 and-9 in both wild-type and mutant p53 colon cancer cell lines. Eur J Cancer 39:1310–1317. doi:10.1016/S0959-8049(03)00204-1
9. Berman E, Werbel LM (1991) The renewed potential for folate antagonists in contemporary cancer chemotherapy. J Med Chem 34:479–485. doi:10.1021/jm00106a001
10. Pinedo HM, Peters G (1988) Fluorouracil: biochemistry and pharmacology. J Clin Oncol 6:1653–1664. doi:10.1200/JCO.1988.6.10.1653
11. Bretner M, Kulikowski T, Dzik JM, Balinska M, Rode W, Shugar D (1993) 2-thio derivatives of durd and 5-fluoro-durd and their 5'-monophosphates: Synthesis, interaction with tumor thymidylate synthase, and in vitro antitumor activity. J Med Chem 36:3611–3617. doi:10.1021/jm00075a016
12. Hurwitz H, Fehrenbacher L, Novotny W, Cartwright T, Hainsworth J, Heim W, Berlin J, Baron A, Griffing S, Holmgren E (2004) Bevacizumab plus irinotecan, fluorouracil, and leucovorin for metastatic colorectal cancer. N Engl J Med 350:2335–2342. doi:10.1056/NEJMoa032691
13. Vincent J, Mignot G, Chalmin F, Ladoire S, Bruchard M, Chevriaux A, Martin F, Apetoh L, Rébé C, Ghiringhelli F (2010) 5-Fluorouracil selectively kills tumor-associated myeloid-derived suppressor cells resulting in enhanced T cell-dependent antitumor immunity. Cancer Res 70:3052–3061. doi:10.1158/0008-5472.CAN-09-3690
14. Macchia M, Barontini S, Bertini S, Di Bussolo V, Fogli S, Giovannetti E, Grossi E, Minutolo F, Danesi R (2001) Design, synthesis, and characterization of the antitumor activity of novel ceramide analogues. J Med Chem 44:3994–4000. doi:10.1021/jm010947r
15. Sayre PH, Finer-Moore JS, Fritz TA, Biermann D, Gates SB, Mackellar WC, Patel VF, Stroud RM (2001) Multi-targeted antifolates aimed at avoiding drug resistance form covalent closed inhibitory complexes with human and *Escherichia coli* thymidylate synthases. J Mol Biol 313:813–829. doi:10.1006/jmbi.2001.5074
16. Tsavaris N, Kosmas C, Vadiaka M, Koufos C (2002) Raltitrexed (tomudex) administration in patients with relapsed metastatic colorectal cancer after weekly irinotecan/5-fluorouracil/leucovorin chemotherapy. BMC Cancer 2:2. doi:10.1186/1471-2407-2-2
17. Scagliotti GV, Parikh P, Von Pawel J, Biesma B, Vansteenkiste J, Manegold C, Serwatowski P, Gatzemeier U, Digumarti R, Zukin M (2008) Phase III study comparing cisplatin plus gemcitabine with cisplatin plus pemetrexed in chemotherapy-naive patients with advanced-stage non-small-cell lung cancer. J Clin Oncol 26:3543–3551. doi:10.1200/JCO.2007.15.0375
18. Jhawer M, Rosen L, Dancey J, Hochster H, Hamburg S, Tempero M, Clendeninn N, Mani S (2007) Phase ii trial of nolatrexed dihydrochloride [thymitaqtm, ag 337] in patients with advanced hepatocellular carcinoma. Invest New Drugs 25:85–94. doi:10.1007/s10637-006-9003-x
19. Appelt K, Bacquet RJ, Bartlett CA, Booth CL, Freer ST, MaM Fuhry, Gehring MR, Herrmann SM, Howland EF (1991) Design of enzyme inhibitors using iterative protein crystallographic analysis. J Med Chem 34:1925–1934. doi:10.1021/jm00111a001
20. Reich SH, MaM Fuhry, Nguyen D, Pino MJ, Welsh KM, Webber S, Janson CA, Jordan SR, Matthews DA (1992) Design and synthesis of novel 6,7-imidazotetrahydroquinoline inhibitors of thymidylate synthase using iterative protein crystal structure analysis. J Med Chem 35:847–858. doi:10.1021/jm00083a007
21. Varney MD, Marzoni GP, Palmer CL, Deal JG, Webber S, Welsh KM, Bacquet RJ, Bartlett CA, Morse CA (1992) Crystal-structure-based design and synthesis of benz[cd]indole-containing inhibitors of thymidylate synthase. J Med Chem 35:663–676. doi:10.1021/jm00082a006
22. Webber SE, Bleckman TM, Attard J, Deal JG, Kathardekar V, Welsh KM, Webber S, Janson CA, Matthews DA (1993) Design of thymidylate synthase inhibitors using protein crystal structures: the synthesis and biological evaluation of a novel class of 5-substituted quinazolinones. J Med Chem 36:733–746. doi:10.1021/jm00058a010
23. Arooj M, Sakkiah S, Ping Cao G, Lee KW (2013) An innovative strategy for dual inhibitor design and its application in dual inhibition of human thymidylate synthase and dihydrofolate reductase enzymes. PLoS ONE 8:e60470. doi:10.1371/journal.pone.0060470
24. Gangjee A, Devraj R, Mcguire JJ, Kisliuk RL (1995) 5-arylthio substituted 2-amino-4-oxo-6-methylpyrrolo[2,3-d]pyrimidine antifo-

lates as thymidylate synthase inhibitors and antitumor agents. J Med Chem 38:4495–4502. doi:10.1021/jm00022a015
25. Fleming FF, Yao L, Ravikumar P, Funk L, Shook BC (2010) Nitrile-containing pharmaceuticals: efficacious roles of the nitrile pharmacophore. J Med Chem 53:7902–7917. doi:10.1021/jm100762r
26. Laurence C, Brameld KA, Graton J, Le Questel J-Y, Renault E (2009) The p k bhx database: toward a better understanding of hydrogen-bond basicity for medicinal chemists. J Med Chem 52:4073–4086. doi:10.1021/jm801331y
27. Teno N, Miyake T, Ehara T, Irie O, Sakaki J, Ohmori O, Gunji H, Matsuura N, Masuya K, Hitomi Y (2007) Novel scaffold for cathepsin k inhibitors. Bioorg Med Chem Lett 17:6096–6100. doi:10.1016/j.bmcl.2007.09.047
28. Gaillard H, García-Muse T, Aguilera A (2015) Replication stress and cancer. Nat Rev Cancer 15:276–289. doi:10.1038/nrc3916
29. Ravichandran J, Gurumoorthy P, Karthick C, Rahiman AK (2014) Mononuclear zinc (ii) complexes of 2-((2-(piperazin-1-yl)ethylimino)methyl)-4-substituted phenols: synthesis, structural characterization, DNA binding and cheminuclease activities. J Mol Struct 1062:147–157. doi:10.1016/j.molstruc.2014.01.026
30. Shankaraiah N, Jadala C, Nekkanti S, Senwar KR, Nagesh N, Shrivastava S, Naidu V, Sathish M, Kamal A (2016) Design and synthesis of c3-tethered 1,2,3-triazolo-β-carboline derivatives: anticancer activity, DNA-binding ability, viscosity and molecular modeling studies. Bioorg Chem 64:42–50. doi:10.1016/j.bioorg.2015.11.005
31. Li X-C, Liu K-G, Qin D-A, Cheng C-C, Chen B-X, Hu M-L (2012) Influence of bromoethyl group on biological activity of 5-fluorouracil prodrug: insights from x-ray crystallography and molecular docking. J Mol Struct 1027:104–110. doi:10.1016/j.molstruc.2012.05.070
32. Nadzri NI, Sabri NH, Lee VS, Halim SNA (2016) 5-fluorouracil co-crystals and their potential anti-cancer activities calculated by molecular docking studies. J Chem Crystallogr 46:144–154. doi:10.1007/s10870-016-0638-y
33. Ding Y, Girardet J-L, Smith KL, Larson G, Prigaro B, Wu JZ, Yao N (2006) Parallel synthesis of 5-cyano-6-aryl-2-thiouracil derivatives as inhibitors for hepatitis C viral NS5B RNA-dependent RNA polymerase. Bioorg chem 34:26–38. doi:10.1016/j.bioorg.2005.10.001
34. Skehan P, Storeng R, Scudiero D, Monks A, Mcmahon J, Vistica D, Warren JT, Bokesch H, Kenney S, Boyd MR (1990) New colorimetric cytotoxicity assay for anticancer-drug screening. J Natl Cancer Inst 82:1107–1112. doi:10.1093/jnci/82.13.1107
35. Wahba AJ, Friedkin M (1962) The enzymatic synthesis of thymidylate i. Early steps in the purification of thymidylate synthetase of *Escherichia coli*. J Biol Chem 237:3794–3801 PMID:13959775
36. Jarmuła A, Frączyk T, Cieplak P, Rode W (2010) Mechanism of influence of phosphorylation on serine 124 on a decrease of catalytic activity of human thymidylate synthase. Bioorg Med Chem 18:3361–3370. doi:10.1016/j.bmc.2010.04.019
37. Schmidt SD, Mazzella MJ, Nixon RA, Mathews PM (2012) Aβ measurement by enzyme-linked immunosorbent assay. Amyloid Proteins Methods Protocols 34:507–527
38. Autodock. Autodock 4.2.6 download page. http://autodock.scripps.edu/downloads/autodock-registration/autodock-4-2-download-page. Access Mar 2016
39. Morris GM, Goodsell DS, Halliday RS, Huey R, Hart WE, Belew RK, Olson AJ (1998) Automated docking using a lamarckian genetic algorithm and an empirical binding free energy function. J Comput Chem 19:1639–1662. doi:10.1002/(SICI)1096-987X(19981115)19:14<1639::AID-JCC10>3.0.CO;2-B
40. Acd/Labs. Acd/chemsketch for academic and personal use. http://www.acdlabs.com/resources/freeware/chemsketch/. Access Mar 2016
41. Pdb. 1ju6. http://www.rcsb.org/pdb/explore/explore.do?structureId=1JU6. Access Mar 2016
42. Expasy. Deepview-swiss-pdbviewer. http://spdbv.vital-it.ch/disclaim.html. Access Mar 2016
43. Pymol. Pymol downloads and documentation. https://pymol.org/dsc/index.php?ip=. Access Mar 2016